Journal Pre-proof

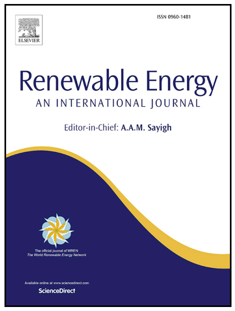

Heat transfer model for energy-active windows – An evaluation of efficient reuse of waste heat in buildings

Behrouz Nourozi, Adnan Ploskić, Yuxiang Chen, Justin Ning-Wei Chiu, Qian Wang

PII: S0960-1481(20)31609-8

DOI: https://doi.org/10.1016/j.renene.2020.10.043

Reference: RENE 14333

To appear in: *Renewable Energy*

Received Date: 9 July 2020

Revised Date: 6 October 2020

Accepted Date: 8 October 2020

Please cite this article as: Nourozi B, Ploskić A, Chen Y, Ning-Wei Chiu J, Wang Q, Heat transfer model for energy-active windows – An evaluation of efficient reuse of waste heat in buildings, *Renewable Energy* (2020), doi: https://doi.org/10.1016/j.renene.2020.10.043.

This is a PDF file of an article that has undergone enhancements after acceptance, such as the addition of a cover page and metadata, and formatting for readability, but it is not yet the definitive version of record. This version will undergo additional copyediting, typesetting and review before it is published in its final form, but we are providing this version to give early visibility of the article. Please note that, during the production process, errors may be discovered which could affect the content, and all legal disclaimers that apply to the journal pertain.

© 2020 Published by Elsevier Ltd.

Journal Pre-proof

Credit author statement

Behrouz Nourozi: Conceptualization; Methodology; Simulation, validation and visualization; Main writer of original draft

Adnan Ploskic: Conceptualization; Methodology; Validation; Supervision; Editing and reviewing

Yuxiang Chen: Methodology; Supervision; Editing and reviewing

Justin Ning-Wei Chiu: Editing and reviewing

Qian Wang: Supervision; Editing and reviewing

Journal Pre-proof

Journal Pre-proof

Heat transfer model for energy-active windows – An evaluation of efficient reuse of waste heat in buildings

Behrouz Nourozi *[1,2], **Adnan Ploskić** [1,3], **Yuxiang Chen** [2], **Justin Ning-Wei Chiu** [4], **Qian Wang** [1,5]

*Corresponding author, Tel.: +46 720051934

Email address: nourozi@kth.se

[1] Division of Sustainable Buildings, School of Architecture and the Built Environment, KTH Royal Institute of Technology, Brinellvägen 23, SE-11428 Stockholm, Sweden

[2] Department of Civil & Environmental Engineering, Innovation Center for Engineering (ICE), University of Alberta, 9211-116 Street NW, Edmonton, Alberta, Canada T6G 2G6

[3] Bravida Holding AB, Mikrofonvägen 28, SE-12637 Hägersten, Sweden

[4] Division of Heat and Power Technology, School of Industrial Engineering and Management, KTH Royal Institute of Technology, Brinellvägen 68, SE-10044 Stockholm, Sweden

[5] Uponor AB, Hackstavägen 1, SE-72132 Västerås, Sweden

Journal Pre-proof

Abstract

Minimizing thermal losses through windows and maintaining large glazing areas to provide adequate natural lighting in residential buildings are essential considerations for modern architecture, sustainability, and indoor comfort. In this study, a detailed heat transfer model for a novel energy-active window (EAW) is developed and validated to rate its thermal performance. An EAW utilizes low-grade heat to reduce building heat losses during the winter season. A thorough literature review was conducted to select the correct heat-transfer correlations for the investigated configuration. A two-dimensional finite differencing scheme was applied to approximate the vertical and horizontal temperature distribution across the EAW. Detailed temperature gradients, across the height and width of the window, were obtained. Thorough sensitivity analyses of the governing parameters were conducted to evaluate the windows' thermal performance. The results indicate that EAWs have the potential to reduce heating power demand by approximately 2.2 $W/m^2_{floor\ area}$ and 1.3 $W/m^2_{floor\ area}$ at outdoor temperatures of -20°C and -5°C, respectively, for buildings with a window-to-floor area ratio of 10%. This potential increases proportionally with the ratio. The highest thermal efficiency of EAW is achieved when the temperature of the supplied air inside the EAW is equal to or above room temperature.

Keywords:

waste heat; energy efficiency; ventilated window; heat transfer; transmittance; energy conservation

Journal Pre-proof

Journal Pre-proof

41 ## Nomenclature

Abbreviations	
EAE	Energy active envelope
EAW	Energy active window
TGW	Triple-glazed window
PCM	Phase change material
Latin letters	
Ra	Rayleigh number, [-]
Gr	Grashof number, [-]
Pr	Prandtl number, [-]
Nu	Nusselt number, [-]
Re	Reynolds number, [-]
Ri	Richardson number, [-]
AR	Aspect ratio of window L/d_s, [-]
a	Absorption coefficient of solar radiation of the pane
b	Window width, [m]
c_p	Specific heat capacity, [$Jkg^{-1}K^{-1}$]
d_s	Slot width, [m]
g	Gravitational acceleration, [ms^{-2}]
h	Heat transfer coefficient, [$Wm^{-2}K^{-1}$]
I	Solar radiation on a pane
k	Thermal conductivity [$Wm^{-1}K^{-1}$]
L	Window height, [m]
L_{char}	Characteristic length, [m]
Q_{gain}	Heat gain, [W]
R	Thermal resistance, [m^2KW^{-1}]
T	Temperature, [°C] (or [K])
t	Window pane (glass) thickness, [m]
U	Thermal transmittance (of window), [$Wm^{-2}K^{-1}$]
v	Air velocity in slots, [ms^{-1}]
Greek letters	
ρ	Density, [kgm^{-3}]
σ	Stefan-Boltzmann constant, 5.67×10^{-8}, [$Wm^{-2}K^{-4}$]
ε	Emissivity of a surface, [-]
μ	Dynamic viscosity, [$kgm^{-1}s^{-1}$]
ν	Kinematic viscosity, [m^2s^{-1}]
β	Thermal expansion coefficient, [K^{-1}]
Δx	Grid size along the window height, [m]
Subscripts	
i	Denoting a term in a sequence along the window height
j	Denoting a term in a sequence across the window section
in	Indoor
out	Outdoor
conv	Convection
cond	Conduction
rad	Radiation
g	Glass (U_g)
w	Window (U_w)
floor	Room floor (area)(A_{floor})
surf	Glass surface
surf, in	Surface of interior glass
s	Slot

1 Introduction

Glazing area in buildings commonly has the lowest thermal resistance compared to the entire building envelope. Lowering the heat transmittance of windows is essential in order to minimize the heating demand of buildings in cold climates. Despite recent developments in research to improve fenestration technology, heat losses from windows are still responsible for approximately 60% of energy loss in residential buildings [1]. Therefore, innovative designs of building fenestration can considerably decrease both building energy demand and peak thermal loads.

Heat transfer between windows and the occupants is conducted in three modes: short-wave solar radiation from outdoors through the window panes, long-wave radiative heat transfer between the window panes and occupants, and convection current caused by cold draughts from the cold surface of windows during winter time. Some of the applied techniques for decreasing the long-wave radiative heat transfer in windows are low-emittance coatings applied on a glass surface, suspended films, photovoltaic, and aerogel glazing [2–5]. Chow et al. [6] evaluated the energy performance of tinted, reflective, and anti-reflective glass in windows to decrease the solar radiative heat transfer from windows. Similarly, the cold draught from the window's surface can be reduced by increasing the thermal resistance of the window. A commonly used technique for this purpose is multilayer glazing [7,8]. In order to further increase the thermal resistance of the window, the gaps between the panes can be vacuumed [9–11], filled with an inert gas with low conductivity [12], or nanoparticle-enhanced PCM [13,14]. Hu et al. [15] investigated a PCM enhanced ventilation window for preheating/precooling ventilation applications. It was reported that, compared to a conventional window, this window had the potential to increase the inlet air temperature by 2°C for 12 hours in a day (heating mode), and maintain the inlet air temperature by average 1.4°C lower during 7 hours in a day.

Another innovative design of windows is to direct fresh or exhaust airflow into the gap between the window panes. This changes the heat transfer type between the window panes in the gaps. Lago et al. [16] and Zeyninejad et al. [17] investigated the thermal performance of a ventilated double-glazed window with a solar reflective film. Lago et al. found that with the optimum spacing of 25 mm, the heat gain to the internal ambient in summer time could be at its minimum. Zhang et al. [18] compared the performance of a conventional triple-glazed window (TGW) with a triple-glazed exhaust air window. This window utilized the low-grade thermal energy from the room exhaust air between the panes. Their results showed that using the triple-glazed exhaust air window could reduce the annual accumulated cooling and heating loads by approximately 25%

and 50%, respectively. Michaux et al. [19] analyzed the thermal performance of an airflow window with conventional double- and triple-glazed windows. They showed a significant reduction in the energy required to heat the fresh supply air to the room by 36–79% for night- and day-time conditions. Liu et al. [20] investigated the energy efficiency and perceived thermal comfort in a space equipped with 15 different window configurations, concluding that ventilated windows had the potential to reduce the heating/cooling demands of buildings and improve the thermal comfort. Lollini et al. [21] studied the efficiency of a dynamic glazing system that actively responds to the external environmental loads. They analyzed the variables that determine the system performance such as U- and g-value. Furthermore, they investigated the glazing type, airflow slot thickness, airflow rate in slots etc. to provide the best performance under different weather conditions and in several building types.

The above-mentioned studies either utilized the fresh supply outdoor air between the glazing to preheat the supply air to the rooms, or used indoor (exhaust) air to heat/cool the window panes during winter/summer. The present paper presents the winter performance of an innovative EAW that utilizes low-grade energy, such as waste heat in a sealed air loop between the window panes. The purpose of using EAW is to utilize waste heat to maintain higher window-surface temperatures in winter. This technology converts conventional passive windows into an energy-active component in addition to previously studied dynamic glazing systems [22]. This will reduce building heating demand, improve the indoor thermal comfort, and alleviate peak heating demands.

1.1 Concept of EAW and heat sources

The investigated EAW was composed of a double-slot glazing configuration and a closed air loop, see Figure 1. The middle glazing assembly was a super-insulated double-pane window filled with argon to minimize the transverse heat transfer from the supply to the return air slot. The sealed closed air loop ensured the avoidance of accumulation of dust on the glass surfaces, and the avoidance of frosting by maintaining a low level of humidity in the air. A built-in heat exchanger combined with a fan underneath the window provided heated air to the slots. A schematic of the analyzed EAW and connections to two possible heat sources, return water from heat emission system, and/or working medium in a heat pump cycle are illustrated in Figure 1a and Figure 1b.

Journal Pre-proof

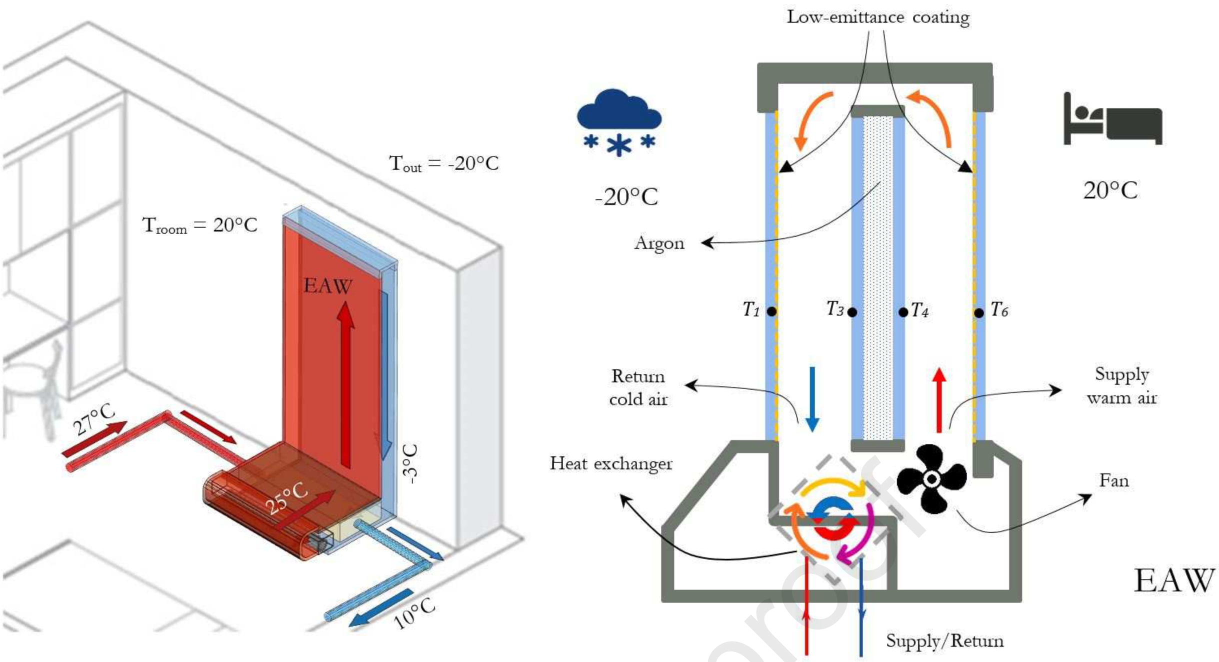

Figure 1a: Schematic of EAW configuration and the connection to heat sources.

104

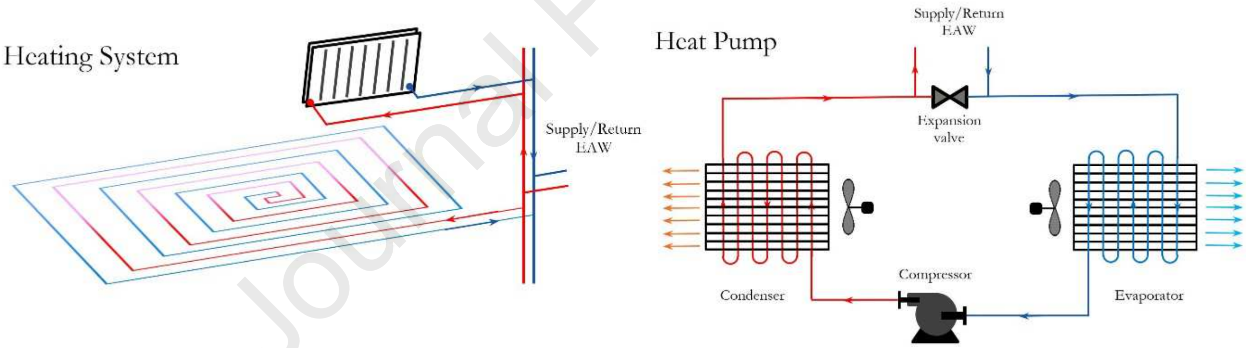

Figure 1b: Two possible low-grade heat sources for EAW, floor heating, and a heat pump cycle.

105 Detailed information about EAW components was reported in a complementary study [23]. The
106 heat transfer model in the cross-section and along the height of the EAW is the focus of this
107 paper. A major challenge of heat transfer modelling in the slots of EAW lies in the convective
108 mechanism. As shown above, the current Nusselt correlations for the laminar flow in narrow
109 asymmetrically heated gaps are limited in the open literature. It is often unknown which type of
110 heat transfer – convective or radiative – controls the heat transfer mechanism through the
111 investigated window type, nor is it certain which convection type (natural, mixed or forced) is
112 predominant between the surfaces. Accordingly, we conducted a thorough study to develop a
113 valid heat transfer model for the energy-active window.

Journal Pre-proof

1.2 Objectives

The main objective of this study is to analyze the thermal performance of an EAW as shown in Figure 1. The goal is to develop a valid simulation model for this novel window type, which is designed and will be field-tested in 2020. The second goal is to select the relevant Nusselt correlations and assess their validity for the investigated configuration. Lastly, the thermal performance of this novel window type is compared with the performance of a corresponding conventional triple-glazed window.

Journal Pre-proof

Journal Pre-proof

2 Methodology with Literature Review

The thermal performance of an energy-active window is evaluated for the heating mode in winter and compared to a conventional triple-glazed window. Heat losses across these two window types are investigated with heat transfer analysis through the windows in the transversal direction. Figure 2 illustrates the detailed heat transfer modes in the cross-section of a conventional TGW and an EAW.

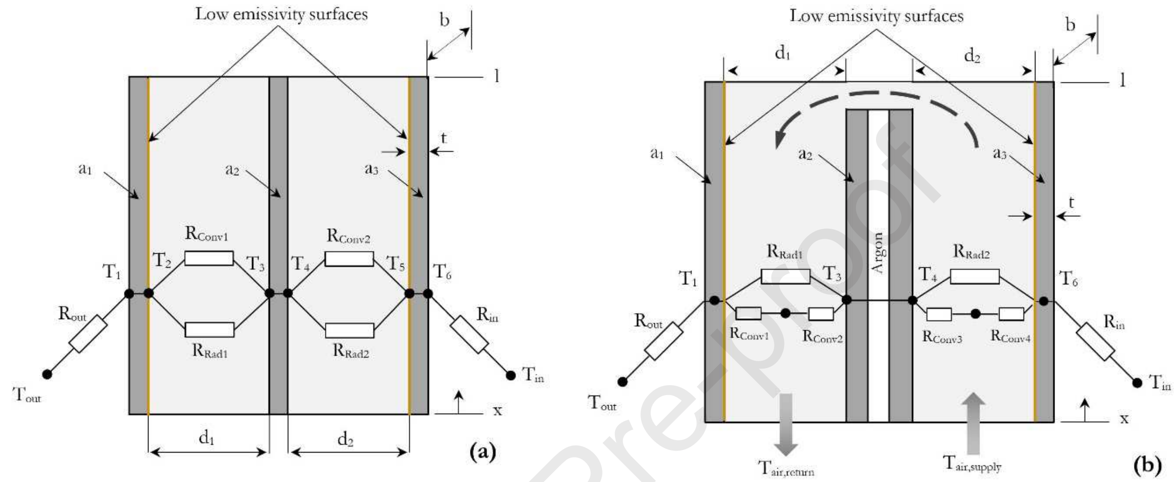

Figure 2: Studied windows, (a) conventional triple-glazed window, (b) energy active window EAW

Equation 1 is obtained by applying the energy balance at each temperature point on the window pane surfaces. This analytical derivation of the heat transfer equations for EAW is based on Schmidt and Johanesson [24].

$$T_j\left(\frac{1}{R_j}+\frac{1}{R_{j+1}}\right)-\frac{T_{j-1}}{R_j}-\frac{T_{j+1}}{R_{j+1}}=a_j I \qquad (1)$$

where T_j is the temperature on each pane surface, I and a_j are solar radiation and the coefficient of solar radiation absorption on each pane, and R_j is the total thermal resistance in each slot, as shown in Equation 2:

$$R_j=\frac{R_{Rad_j}R_{Conv_j}}{R_{Rad_j}+R_{Conv_j}} \qquad (2)$$

Table 1 presents the mathematical and empirical equations used for heat transfer approximation in this study. The validity range for each equation and the conditions in which they are utilized are provided in Table 1:

Journal Pre-proof

Table 1: Mathematical and empirical equations used for calculation of heat transfer coefficients used in Equation 1 and 2.

Reference	Equation	Equation No.		Validity
	$h_{conv} = Nu \, {k_{gas}}/{L_{char}}$	(3)	Convective heat transfer coefficient	
	$h_{rad} = \dfrac{\sigma\left(T_{surf,1}+T_{surf,2}\right)\left(T_{surf,1}{}^{2}+T_{surf,2}{}^{2}\right)}{\dfrac{1}{\varepsilon_{surf,1}}+\dfrac{1}{\varepsilon_{surf,2}}-1}$	(4)	Radiative heat transfer coefficient between two panes of different emissivity	
	$h_{cond} = {k_g}/{t}$	(5)	Conductive heat transfer coefficient through a pane	
	$Pr = c_{p,gas} \, {\mu_{gas}}/{k_{gas}}$	(6)	Prandtl number	
	$Gr = \dfrac{g\beta_{gas}\left(T_{gas}-T_{surf}\right)L^{3}}{v_{gas}{}^{2}}$	(7)	Grashof number	
	$Ra_L = GrPr = \dfrac{\rho^2 g\beta\Delta T L^3 c_p}{\mu k}$	(8)	Rayleigh number for the inner window surface	
Zhao et al. [25]	$Nu = \left(1+4.4265\times10^{-4}\times\left(\dfrac{Ra_L}{AR}\right)^{1.36869}\right)^{0.326071}$	(9)	Nusselt number for large aspect ratio (AR) vertical cavities. Used here for calculating natural convective heat transfer coefficient between window panes	$30 \leq AR \leq 110$ $Re_L < 20000$
Churchill & Chu [26]	$Nu_{in} = \left[0.825+\dfrac{0.387Ra_L{}^{1/6}}{\left[1+\left({0.492}/{Pr_{in}}\right)^{9/16}\right]^{8/27}}\right]^{2}$	(10)	Nusselt number for the inner window surface facing room	Entire range of Rayleigh number
Bar-Cohen & Rohsenow [27]	$Ra_{d_s} = \dfrac{\rho^2 g\beta\Delta T d_s{}^4 c_p}{\mu k L}$	(11)	Modified Rayleigh number for slots used in Equation 12	
Bar-Cohen & Rohsenow [27]	$Nu = \left[{144}/{\left(Ra_{d_s}\right)^2}+{2.873}/{\left(Ra_{d_s}\right)^{1/2}}\right]^{-1/2}$	(12)	Nusselt correlation for vertical asymmetrically heated isothermal parallel plates	
Edwards et al. [28]	$Nu = 7.54+\dfrac{0.03\left(D_h/L\right)RePr}{1+0.016\left[\left(D_h/L\right)RePr\right]^{2/3}}$	(13)	Laminar forced convection between isothermal parallel plates	$Re_{D_h} < 2800$
Stephan [29]	$Nu = 7.55+\dfrac{0.024\left(RePrD_h/L\right)^{1.14}}{1+0.0358Pr^{0.81}\left[RePrD_h/L\right]^{0.64}}$	(14)	Laminar forced convection between isothermal parallel plates	
Granryd [30]	$Nu = 7.54+\dfrac{0.0289\left(RePrD_h/L\right)^{1.37}}{1+0.0438\left(RePrD_h/L\right)^{0.87}}$	(15)	Laminar forced convection between isothermal parallel plates	$Re_{D_h} < 2500$

Journal Pre-proof

2.1 Boundary conditions

In this study, indoor and outdoor air temperatures are assumed to be at +20°C and -20°C, respectively. Furthermore, the sensitivity analysis of an outdoor temperature between -30°C and +10°C on the window U-value is also performed. Intermittent solar radiation especially during winter season in Sweden, and low outdoor temperatures that happen during night are more critical for examining the window performance with the absence of solar radiation. The gas utilized in the slots for the TGW is krypton. For EAW, air is used as heat transfer fluid in the slots. The window parameters and additional boundary conditions are presented in Table 2.

Table 2: Parameters and boundary conditions used in EAW simulations

Parameter	$(L \times b \times t)$	d_s	U_g	h_{out}	$\dot{m}_{air}$	T_{in}	$\mathrm{T}_{\mathrm{out}}$	ε
Unit	m^3	m	$Wm^{-2}K^{-1}$	$Wm^{-2}K^{-1}$	kgs^{-1}	°C	°C	[-]
Value	1×1×0.04	0.01	5.75	34	0.003	20	-20	0.84 (and 0.12)

2.2 Heat transfer from window interior and exterior surfaces

The heat transfer mechanism on the interior and exterior window surfaces are radiation and convection. Thus, radiative and convective heat transfer correlations for vertical plates are adopted in this paper. The air flow type on the exterior window surface depends on the weather conditions. The total thermal transmittance across the window is mainly dependent on the largest thermal resistance, as they are in series. Therefore, different values for the outdoor heat transfer coefficient, which has a larger value than other sections in the window, induce a negligible difference, as shown in the results section. A commonly used value of peak load calculation for the exterior heat transfer coefficient, h_{out}, in winter is used in this investigation [31].

The empirical correlation of the average Nusselt number for natural convection over a vertical surface by Churchill and Chu [26], shown in Equation 10, is considered. This equation is valid for the entire range of Rayleigh number. Equation 3, presented in its general form, is used to approximate the convective heat transfer on the interior window surface.

Finally, the U-value of the window is evaluated with energy balance as shown in Equation 16.

Journal Pre-proof

$$\frac{U_w}{h_{in}} = \frac{T_{in} - T_{surf,in}}{T_{in} - T_{out}} \tag{16}$$

where $T_{surf,in}$ is the temperature of inner glazing facing room and h_{in} is the heat transfer coefficient on this surface.

2.3 Heat transfer between window panes

The radiative heat transfer coefficients between the window panes and the conductive heat transfer coefficient in the window panes are calculated with Equations 4 and 5; see Table 1 for both window types. The convective heat transfer modeling due to differences in the air flow in the TGW and EAW are presented in the Subsections 2.3.1 and 2.3.2, respectively.

2.3.1 Triple-glazed windows

Heat transfer across the window depends on three modes of convection and radiation in the slot and conduction in the window panes. The gas conduction in the slots can be neglected since the Rayleigh number is larger than the critical limit [32–34]. The critical Rayleigh number in rectangular vertical cavities exposed to a horizontal heat flow is 1000; below this number, the buoyancy forces cannot overcome the viscous forces [32]. Rayleigh numbers for the studied TGW are 1280 and 1390 for the inner and outer slots, respectively. This explains that heat transfer due to advection is dominant compared to conduction.

For natural convection between window panes, the spacing between the panes serves as the characteristic length. Air properties used in equations are chosen at respective air bulk temperatures between -40°C and +40°C. The slots between the TGW panes are sealed at the bottom and top and the encased gas is treated as an enclosed cavity. Correlations for the convective heat transfer in narrow cavities with large aspect ratios (AR) optimally predict the heat transfer in slots between the window panes. The Nusselt relation suggested by Zhao et al. [25] covers ARs of $30 \leq AR \leq 110$ and is used here to estimate convective heat transfer in the glazing cavities where AR= 100 (see Equation 9).

2.3.2 Energy-active windows

Unlike the conventional triple-glazed window, the air flow between panes in the EAW is driven by an integrated fan below the window, cf. Figure 1. The injected air velocity in this study is approximately 0.24 m/s, which is equal to air mass flowrate of 3×10^{-3} kg/s in the slots. This air

Journal Pre-proof

Journal Pre-proof

flow rate results in laminar flow with Reynolds number of 300 to 400 due to fluctuation in temperatures. The glass surface exposed to the fan-driven air flow transfers heat with both natural and forced convection. The dominance of each type is shown through the Richardson number $Ri = {Gr}/{Re^2}$ which is studied for similar cases [35–38]. These literatures suggested $Ri = 0.25$ and $Ri = 4$ as the limits for forced, mixed, and natural convection in these studies. For Richardson numbers above 4, inertia forces are negligible and natural convection is dominant. Forced convection is the major heat transfer mechanism for Richardson numbers below 0.25; therefore, buoyancy forces are omitted in this regime. At the intermediate range, the mixed convection is dominant in the slots, and the Nusselt number is calculated with Equation 17 [28,31].

$$Nu_{mixed} = \left(Nu^3_{forced} + Nu^3_{natural}\right)^{1/3} \tag{17}$$

Three commonly used Nusselt correlations for laminar forced convective heat transfer for parallel plates are listed in Equations 13, 14, and 15 in Table 1. These relations were originally developed for prediction of convective heat transfer between symmetrically heated parallel plates with uniform surface temperature. In this study, window pane (surface) temperatures are asymmetrically heated due to a large indoor and outdoor temperature difference and due to the injected hot air flow. This results in air slots enclosed by asymmetric glazing temperatures. As a simplification, the surface temperature of each glazing is assumed to be uniform. Shah and London [39] considered this important difference in the boundary condition and suggested the values for the fully developed Nusselt numbers for symmetrically and asymmetrically heated parallel plates with uniform surface temperatures, see Equation 18.

$$\begin{cases} \text{If } T_{w_1} \neq T_{w_2} & Nu_1 = Nu_2 = 4 \\ \text{If } T_{w_1} = T_{w_2} & Nu_T = 7.54070087 \end{cases} \tag{18}$$

As can be seen, the fully developed Nusselt number for asymmetrical temperature conditions was significantly lower than that of symmetrically heated wall temperatures. The Nusselt correlations shown in Equations 13, 14, and 15 consist of a constant value (7.54 and 7.55), followed by a correction term for hydro-dynamical and thermal undeveloped flows. Therefore, these constant values of 7.54 in Equations 13 and 15 and 7.55 in Equation 14 are changed to 4 to more correctly consider the effects of asymmetrically heated boundaries, as shown in Equation 18. The modified

Equations 13–15 are presented in Figure 3 for the relevant flow velocities and Reynolds numbers in the EAW.

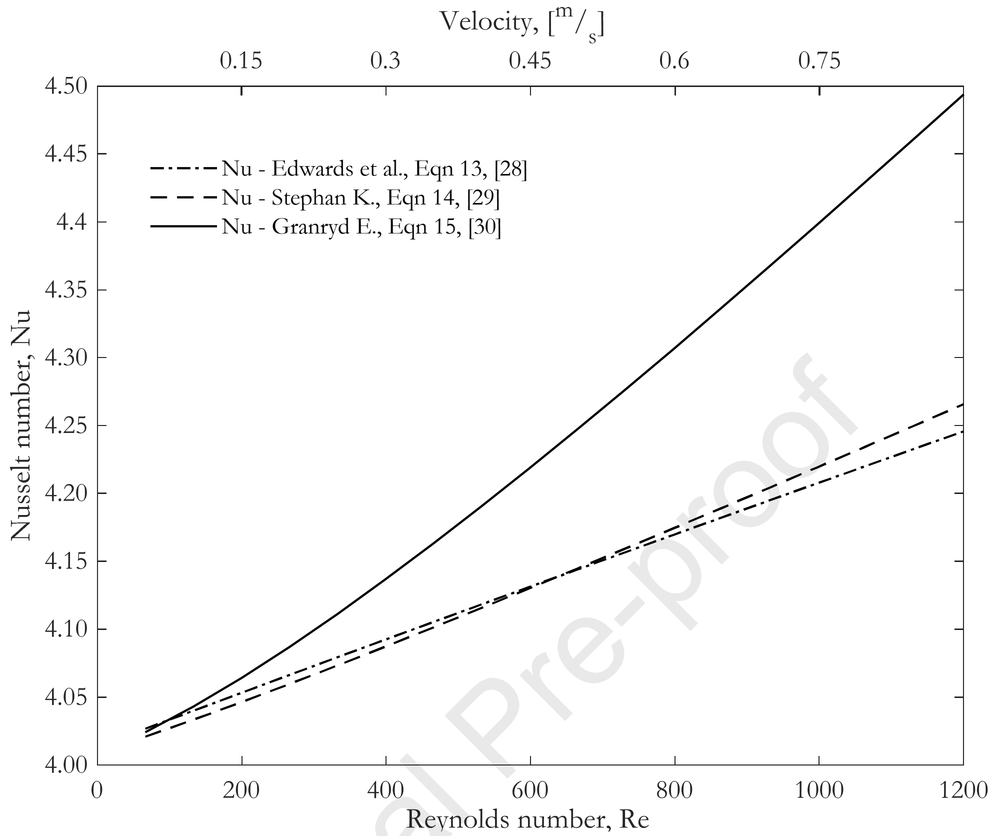

Figure 3: Nusselt correlations for laminar forced convective heat transfer for parallel plate flow

Figure 3 shows that the difference between the predicted Nusselt numbers by Equations 13, 14, and 15 was negligible for Reynolds numbers between 50 and 1200. For the air velocity of 0.24 m/s and the corresponding Reynolds number (approximately 300) in this study, the difference among Equations 13–15 was less than 1%. Thus, Equation 13 by Edwards et al. [28] is put forward in this study.

Journal Pre-proof

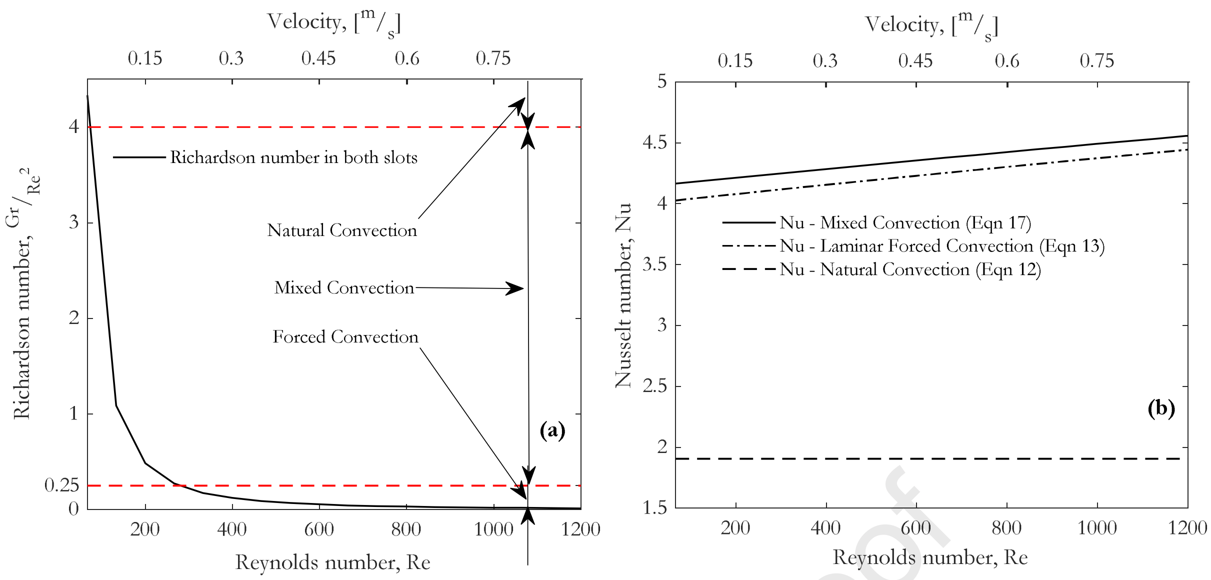

Figure 4: Convective heat transfer type according to the Richardson and Reynolds numbers in slots

As discussed above, the choice of correct correlations for natural, mixed and forced convection in the slots is evaluated using the Richardson number (Gr/Re^2). Figure 4a illustrates the corresponding Richardson number for each convection type in an expectable range for relevant airflow velocity and Reynolds number in the slots. It can be seen that for Reynolds numbers higher than 270, laminar forced convection was the dominant heat transfer mechanism, which means that buoyancy forces are negligible. Figure 4b presents the Nusselt correlations given by Equations 12, 13, and 17 for natural, laminar forced, and mixed convection, respectively. Since the Reynolds number of the supplied air flow to the slots is above 300, all calculations of convective heat transfer in the slots of EAW can be assimilated to forced convection.

In the case of very low airflow velocities in the slots, natural convection in the slots are to be considered with the Nusselt correlation suggested by Bar-Cohen and Rohsenow [27]. Thus, Equation 12 is used to calculate the Nusselt number for vertical isothermal parallel plates with asymmetric temperatures for natural convection in the slots.

2.4 Prediction of vertical temperature distribution in slots

A two-dimensional finite differencing scheme is used to approximate the vertical and transverse temperature distribution between the window panes. Since the airflow in the slots is only affected by the upstream properties, an upwind differencing scheme is used for the thermal modeling of the air, as presented in Equation 19 [40].

Journal Pre-proof

$$T_{air}^{i} = \frac{\dot{m}c_{p.air}T_{air}^{i-1} + b\Delta x\sum_{j}\left(T_{surf}^{i,j}h_{conv}^{i,j}\right)}{\dot{m}c_{p.air} + b\Delta x\sum_{j}\left(h_{conv}^{i,j}\right)} \tag{19}$$

where $\dot{m}$ is the air mass flowrate, $h_{conv}^{i,j}$ is the convective heat transfer coefficient in previous control volume, $h_{conv}^{i,j}$ is the heat transfer coefficient with the window panes across the window, Δx is the grid size along the window height, b is the window width, and T_{surf}^{i} is the temperature at window panes across the window cross-section.

Equations 20 and 21 are utilized to calculate panes temperature along the height of the window.

$$T_{surf}^{i,j} = \frac{k\frac{bt}{\Delta x}\left(T_{surf}^{i-1,j} + T_{surf}^{i+1,j}\right) + b\Delta x\left(T_{surf}^{i,j}h_{rad}^{i,j} + T_{air}^{i,j}h_{conv}^{i,j} + T_{in/out}h_{in/out}\right)}{2k\frac{bt}{\Delta x} + b\Delta x\left(h_{rad}^{i,j} + h_{conv}^{i,j} + h_{in/out}\right)} \tag{20}$$

$$T_{surf}^{i,j} = \frac{k\frac{bt}{\Delta x}\left(T_{surf}^{i-1,j} + T_{surf}^{i+1,j}\right) + b\Delta x\left(T_{surf}^{i,j-1}h_{rad}^{i,j-1} + T_{air}^{i,j}h_{conv}^{i,j} + T_{surf}^{i,j+1}h_{rad}^{i,j+1} + T_{argon}h_{argon}\right)}{2k\frac{bt}{\Delta x} + b\Delta x\left(h_{rad}^{i,j-1} + h_{conv}^{i,j} + h_{rad}^{i,j+1} + h_{argon}\right)} \tag{21}$$

where $T_{in/out}$ and $h_{in/out}$ are the indoor/outdoor temperatures and the heat transfer coefficients at the interior/exterior glazing, respectively. $h_{argon} = 2.95 \,{}^{W}\!/_{m^2K}$ denotes the total transmittance of the middle glazing assembly. T_1 and T_4 are obtained with Equation 20, and T_2 and T_3 are obtained with Equation 21.

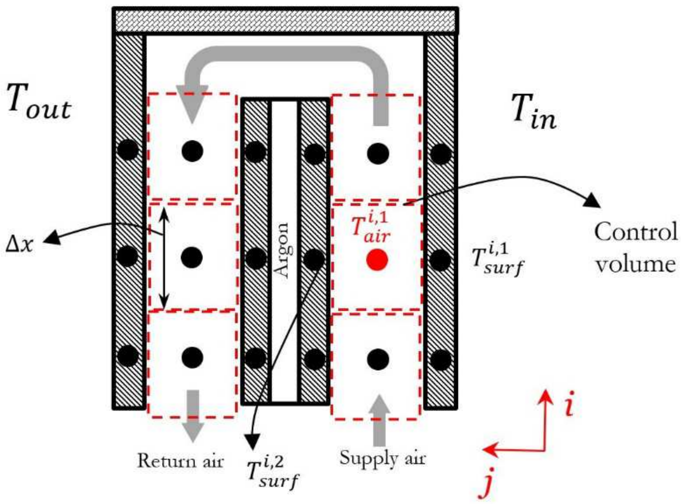

Figure 5: Discretization of air slots along the window height

Journal Pre-proof

As shown in Figure 5, the window is discretized along the height and energy Equations 19, 20, and 21 are used over each air and pane control volume. The minimum number of mesh along the height of the window for mesh independence amounts to 150 from this study. The radiative and convective heat transfer coefficients used in both equations are calculated as described in Sections 2.2 and 2.3.

2.5 Validation

In the following two subsections, the validity of the developed modeling approach is verified by comparison with available data from previous studies. The conventional TGW model is validated as a base model for the EAW. Nusselt correlations used in the models are discussed and the front and end boundary conditions are compared against measured data for both window types.

2.5.1 Validation of TGW simulation

The simulated heat transfer for the triple-glazed window is validated against measured data reported by Larsson et al. [41]. Two different indoor and outdoor temperature conditions are investigated and the results are shown in Figure 6. The temperature gradients across the cross-section of a one-meter-high TGW with krypton in 12 mm wide slots is shown. Temperatures T_1–T_6 comply with the temperature points shown in Figure 2a. The window height is 1m, which means the aspect ratio is 83.

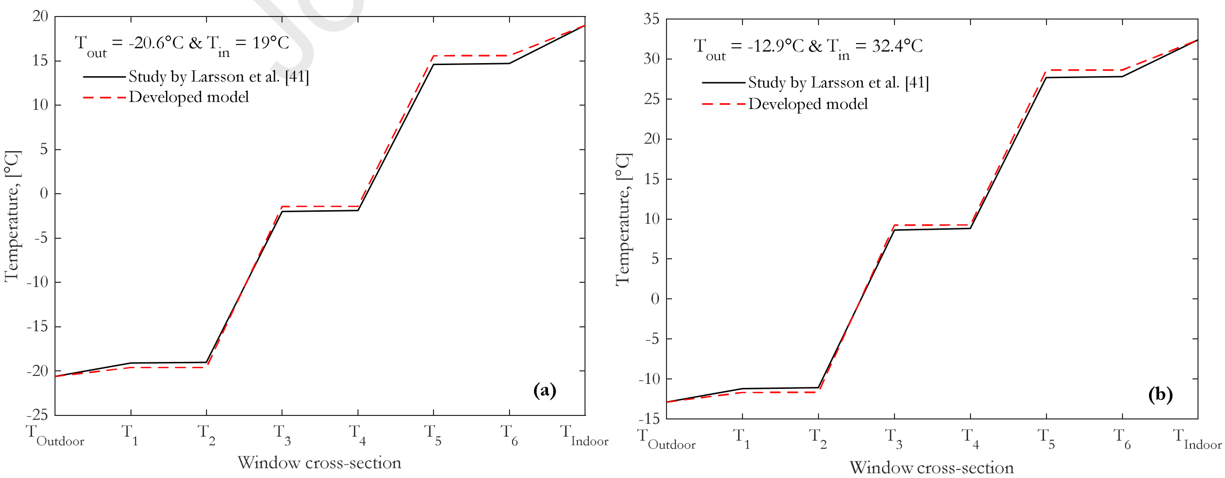

Figure 6: Comparison of the developed model with the study by Larsson et al. [41] for two outdoor and indoor temperatures. The AR =83.

Journal Pre-proof

The simulated temperature change across the window shows good agreement with the measured one by Larsson et al [41]. The maximum deviations between the two methods are 0.9 °C and 1°C (2.9% and 5.7%), respectively, for the two studied temperature conditions.

The deviations in the temperature profiles in Figure 6 are due to different Nusselt correlations. Larsson et al. calculated the Nusselt number for a cavity configuration using the Nusselt correlation suggested by Elsherbiny et al. [42]. In the present study, however, the Nusselt correlation suggested by Zhao et al. [25] has been used because it is more suitable for convective heat transfer in the slots. Correlations suggested by Elsherbiny et al. result in higher Nusselt values for larger Rayleigh numbers and aspect ratios compared to the correlation proposed by Zhao et al. The higher accuracy of the correlations was previously elaborated and thoroughly discussed by Zhao et al. [25].

2.5.2 Validation of the developed EAW simulation model

The thermal performance of a prototype of an EAW was previously investigated by Bergman [43]. Bergman measured the air flow and inner glazing temperatures of an EAW installed in a demonstration building. The results of these temperature measurements for various airflow rates are compared to the simulated values in this study and are presented in Figure 7.

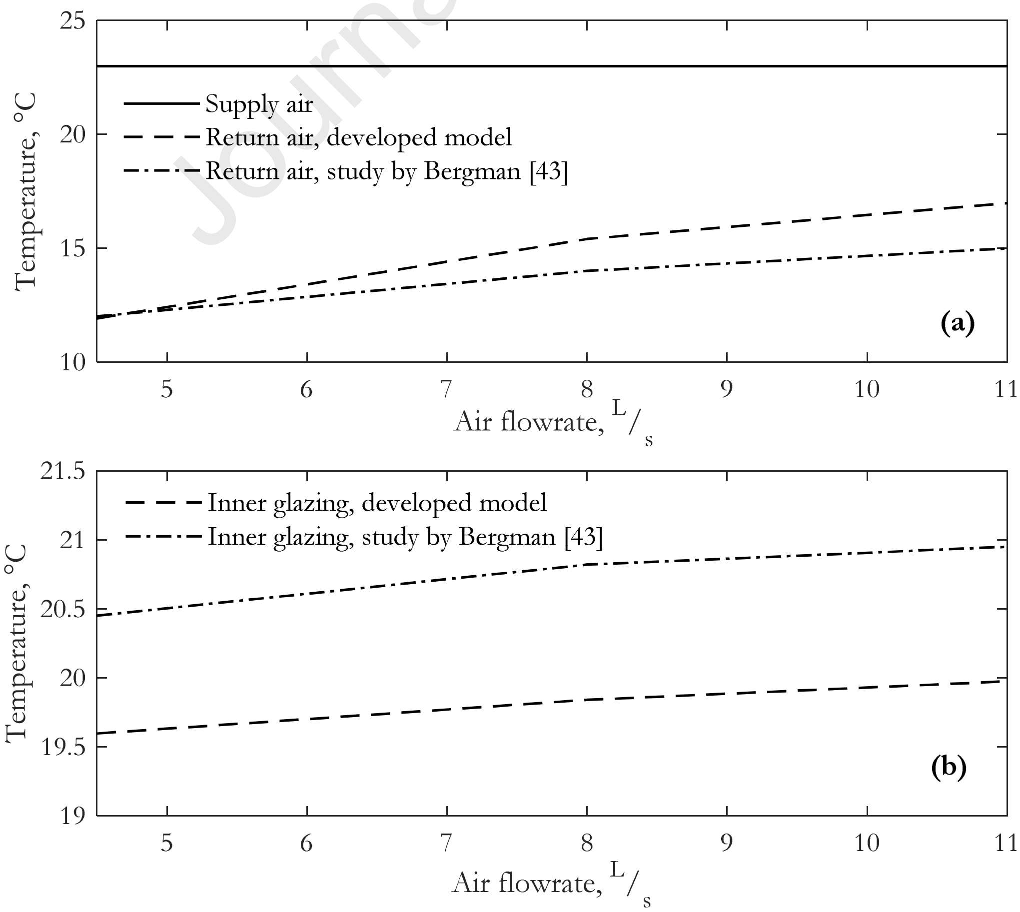

Figure 7: Simulated and measured [43] return air and inner glazing temperatures for EAW.

The supply air temperature for present simulation and previous demonstration was 23 °C. The injected airflow rate to the slots varied between 4.5-11 L/s in the study by Bergman [43]. The temperature of the inner glazing was measured at four locations of the pane to identify the transverse and vertical temperature gradients. Figure 7a shows the measured and the simulated return air temperatures as they diverge with the increasing airflow rate. Comparison showed that the measured and simulated temperatures for the low airflow rate (4.5 L/s) are in excellent agreement, and the maximum deviation was 2 °C, which corresponds to 12%, at an airflow rate of 11 L/s. Figure 7b shows the measured and simulated inner glazing temperatures at the studied air flowrate of 4.5-11 L/s. The maximum temperature difference between these two methods was approximately 0.7 °C, which corresponds to 4% at flowrate of 11 L/s. In this study, airflow rate of 2.4–5.7 L/s is investigated and the maximum deviation in this range is 3%. This comparison verifies that the selected heat transfer equations and the developed simulation model are valid.

Journal Pre-proof

Journal Pre-proof

3 Results

The thermal performance results of the mentioned EAE were presented by comparing them with a conventional TGW. The key parameters of windows were identified and their impact on the performance of both window types was studied.

3.1 EAW performance

Figure 8 depicts the air and pane temperature distribution along the EAW height. The indoor and outdoor temperatures were 20°C and -20°C, respectively, as introduced in Section 2. Supply air temperature to the slot was 20°C and the return air temperature at the bottom of window, as can be seen, was -5°C.

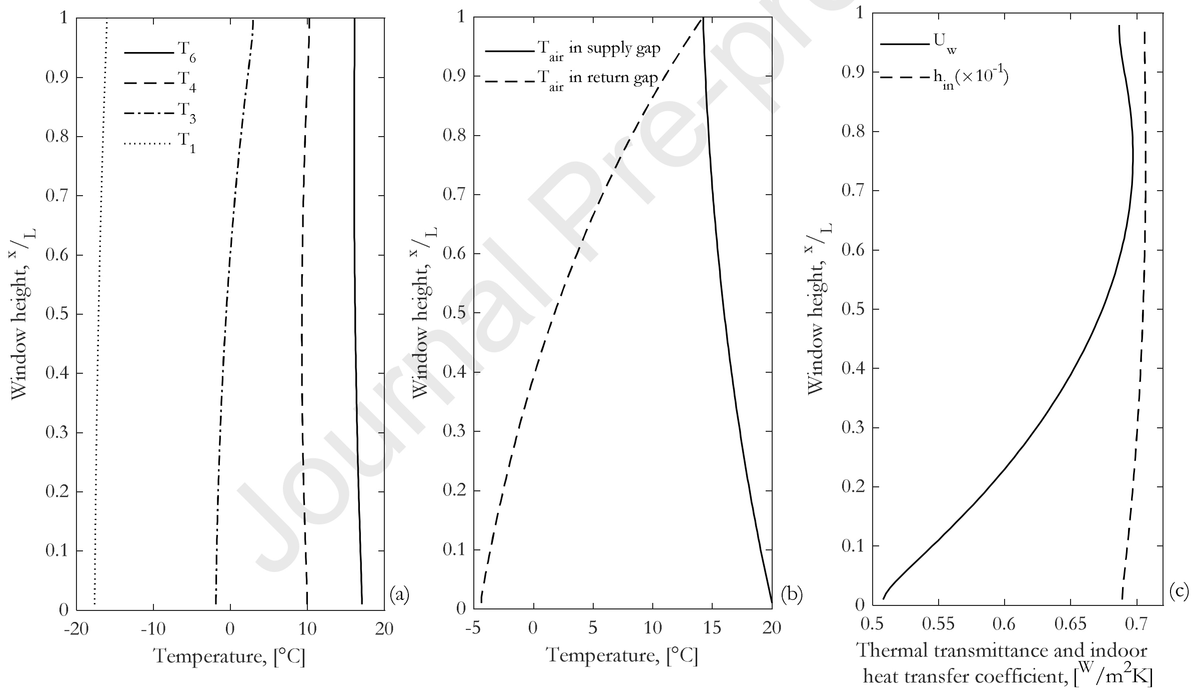

Figure 8: Air and panes temperature and U-value along the height of the EAW

The supply and return air temperature in the slots is shown in Figure 8(a). The air temperature at the upper window edge was 14°C and decreased to -5°C at the bottom of the return slot facing outdoors. The glass temperatures are shown in Figure 8(b), where temperatures T_1, T_3, T_4, and T_6 comply with the surface temperatures presented in Figure 1. Surface temperatures T_4 and T_6 were almost constant along the window height compared to the other two (T_1 and T_3). Figure 8(c) shows the representative U-value along the window height. Due to different inner glazing temperature and indoor heat transfer coefficient, the U-value varied from 0.5–0.7 W/m^{2}K. The indoor heat transfer coefficient, h_{in}, varied from 6.8–7.1 W/m^{2}K.

3.2 Impact of slot size

Within the cross-section of windows, the vacuum or gas-filled gaps have the largest thermal resistance compared to the window panes. Therefore, the size of the gap and the properties of the encased gas influence the total heat transfer through the window cross-section.

Figure 9 shows the impact of sizing of slots of the EAW on the U-value along the window height and the return air temperature from the slots. Three cases of EAW designs with 10mm, 12.5mm, and 15mm slot width in a range of injected air temperatures were simulated. By increasing the slot size for every supply air temperature, the return air temperature also increased. In contrast, the average U-value along the window height decreased when supply temperatures were raised. However, at a supply air temperature of approximately 18°C, the effect of slot size on the U-value was negligible. Therefore, the U-value decreased in wider slots and for supply air temperatures below 18°C, and increased for wider slots and for supply air temperatures above 18°C.

Journal Pre-proof

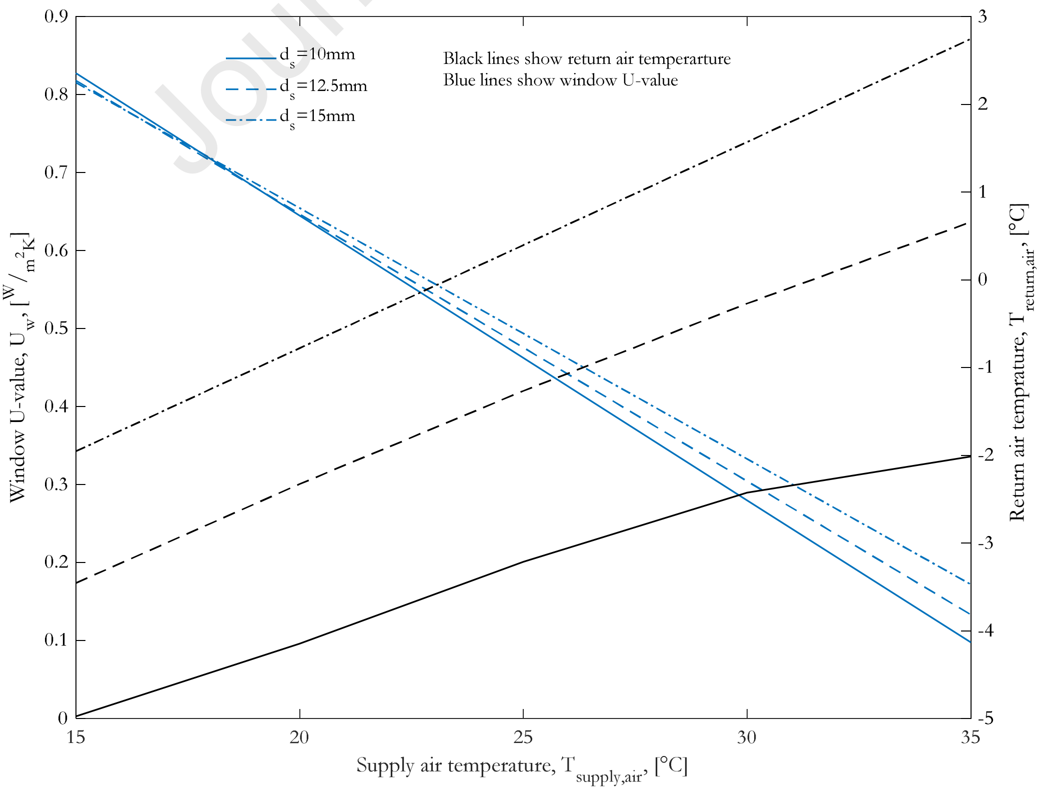

Figure 9: Impact of slot size on air temperature in the slots and U-value

3.3 Impact of temperature difference

The window U-values presented by window manufacturers are commonly defined for a specific temperature difference on the two sides of the window surfaces. In practice, these values vary as the outdoor temperature changes. Figure 10 indicates such influence of outdoor temperature on the U-value and the return air temperature in the slots. These results are presented for four different supply air temperatures to the slots. Note that the indoor temperature remained constant (20°C) for the entire simulations. Therefore, the temperature difference at the two sides of the window varied between 10°C and 50°C.

As can be seen, the return air temperature constantly increased by the increased outdoor temperature. This trend was not affected by the supply air temperature. However, the average U-value of the window along the height was dependent on the supply air temperature. For supply air temperatures below 20°C, the U-value increased by increasing the outdoor temperature. For supply air temperatures above 20°C, the U-value decreased as the outdoor temperature increased.

Journal Pre-proof

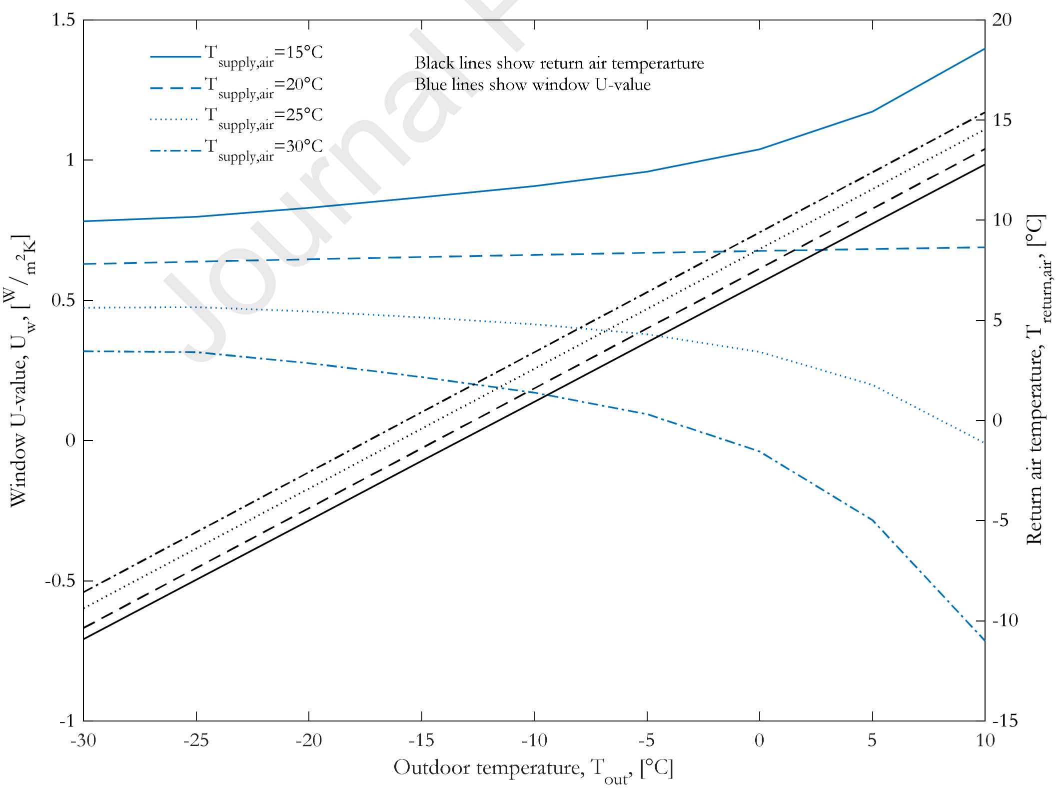

Figure 10: Impact of outdoor temperature on EAW U-value, T_{in} = 20°C

3.4 Impact of airflow rate on EAW performance

The thermal performance of EAW could also be affected by the injected airflow rate to the slots. Furthermore, higher velocities due to increased airflow rates will affect the rate of convective heat transfer in the slots. Thus, Figure 11 illustrates the effect of the injected air velocity on the EAW thermal transmittance and the return air temperature.

The thermal performance of EAW was investigated by injecting warm air (20°C) with velocities ranging from 0.24–0.57 m/s, which corresponds to air flowrates of 3×10^{-3}–7×10^{-3} kg/s. As can be seen, higher air velocity in the slots resulted in an increase in the return air temperature to the heat exchanger at the bottom of EAW. The slope of the black lines increased for higher air velocities, which means that the return air temperature increased proportionally with the supply air velocity.

However, the U-value (blue lines) decreased with both supply air velocity and temperature. In other words, higher air velocities in the slots at constant supply temperatures resulted in lower thermal transmittance. Similarly, injecting the air with higher temperatures to the slots resulted in lower average U-values along the window height.

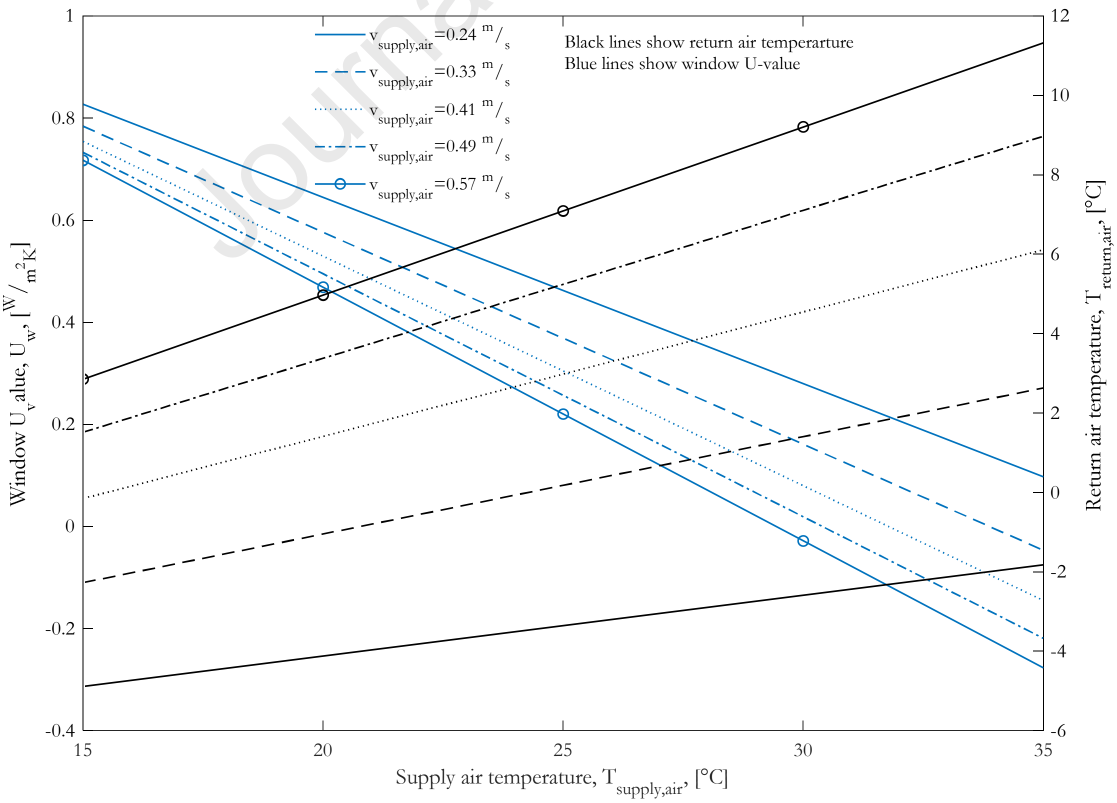

Figure 11: Impact of air velocity in slots on window U-value and return air temperature for air velocities between 0.24 and 0.57 m/s (air flowrates of 3×10^{-3} – 7×10^{-3} kg/s)

4 Discussion

In this paper, the heat transfer in an energy-active window (EAW) has been investigated. The window was heated by a tempered internal air flow that was circulated between window panes. Results have shown that the total heat transfer rate through this window type was mostly controlled by the thermal radiation between the panes. However, the heat transfer rate between the injected warm air and the panes was predominantly governed by the convection that has been evaluated in this study. For convectional windows, the narrow distance between the window panes and the height of the window resulted in high aspect ratios. Nusselt correlations for such configurations are rare in the available literature. In this study, appropriate Nusselt correlations from two previous studies were used to model the heat transfer through conventional triple-glazed windows. The obtained results were compared with results from a previous study. A close agreement between the simulated and the previous data was obtained.

Nusselt correlations for narrow open cavities with different surface temperatures and low Richardson numbers are also rare in the available literature, which made modeling work challenging. In this paper, well-known Nusselt correlations for laminar forced convection were adjusted for use in EAWs, whose panes had different surface temperatures. Because of this, the constant value in the original Nusselt correlations was changed according to recommendations in the literature. Furthermore, a detailed mapping of the convection type (natural, mixed or forced) inside the window slots was performed to correctly evaluate the heat transfer characteristics in these parts.

As presented in Figure 8, the airflow temperature dropped more significantly in the return slot compared to the supply slot. This showed that the heat transferred from the EAW to outdoor was largely higher than the heat transfer to an indoor environment. Therefore, low-grade heat, such as waste heat, should preferably be used for heat supply to EAW. Another reason for such temperature profile for the air along the window height is the high thermal insulation of the middle section, in which argon is utilized. As a result, T_4 and T_6 profiles were less affected by the air temperature in the return slot.

The present study did not examine the effects of flow disturbances on the inner glazing towards the room due to factors such as occupants' movements, room heaters, and curtains. Thus, the indoor heat transfer coefficient was rather constant along the window height. This, together with used constant heat transfer coefficient on the glazing towards outdoor, resulted in a fairly uniform temperature distribution along the window panes.

Journal Pre-proof

The thermal performance of the EAW was quantified as an average U-value along the window height. The U-value was impacted by several parameters that were given special notice in Figure 9, Figure 10 and Figure 11. These figures generally showed that by increasing the supply air temperature the U-value dropped. This was independent of variations in the slot gap, outdoor temperature, and the air velocity in the slots. However, if the supply air temperature was equal to the indoor temperature, the U-value was not affected by the outdoor temperature. Thus, an important conclusion that could be drawn from Figure 10 is that to ensure low U-values at different outdoor temperatures, the supply air temperature to EAW must be above the indoor temperature, which was 20 °C in this study. The negative U-values in Figures 9, 10, and 11 represent the heat transfer to indoor. In this situation, the window acts as a heat emitter for the indoor environment since its surface temperature is higher than the room temperature.

The return air temperature from EAW can be used to evaluate the rate of the used heat from a waste heat source and the heat gain by the window. As can be observed in Figure 9, Figure 10, and Figure 11, the return air temperature was raised by increasing the supply air temperature to EAW, the injected air velocity, and the slot size.

According to the latest Swedish building regulation release provided by Boverket (The Swedish National Board of Housing, Building and Planning), the window glazing area should be at least 10% of the floor area [44]. The studied EAW case here, shown in Figure 8, can be compared to a conventional window with nominal U-value of 1.2 W/m^2°C at two outdoor temperatures of -20°C and -5°C, using Equation 22. The room heat gains by replacing the conventional window with EAW will be 13–22 W for each window unit area. Assuming a window-to-floor area ratio of 10% and given the indoor/outdoor conditions, the evaluated EAW has a potential to reduce the room heating demand by 1.3-2.2 W/m$^2_{\text{floor area}}$ for the mentioned outdoor temperatures.

$$Q_{gain}/A_{floor} = \left(U_{TGW} - U_{EAW}\right)\left(T_{in} - T_{out}\right) A_w/A_{floor} \tag{22}$$

The real-life implementation of the studied window has not yet been evaluated and its thermal energy and power implications have not been fully attained. Therefore, a pilot study will be conducted to evaluate the feasibility, cost, and other implications in order to improve the concept design prior to further industrialization.

Journal Pre-proof

5 Conclusions

In this study, thermal performance of a novel energy-active window (EAW) type was evaluated and compared with a conventional triple-glazed window. According to the previous studies, the Nusselt correlations used for evaluating the laminar forced convective heat transfer in narrow slots with asymmetric temperatures result in considerably lower values compared to symmetric conditions. Moreover, the unique configuration of the studied window with specific airflow regime mandated use of modified correlations to simulate the heat transfer mechanism correctly. Therefore, a detailed heat transfer model was developed and validated for the investigated configuration of EAW. The major findings are:

- The heat source for the energy-active window must come from a low-grade thermal source or waste heat since a large share of supplied heat to the EAW is transferred to the outdoor.
- Thermal radiation is the dominant heat transfer mechanism for both the EAW and the conventional triple-glazed window.
- The Nusselt number for parallel plates with asymmetric surface temperatures is approximately 1.9 times lower than for symmetric (same) surface temperatures. This fact should be considered carefully when designing heat exchangers with different surface temperatures, as was shown in this study.
- At various outdoor and supply temperatures, the effect of slot size is negligible. For an example, at outdoor and supply temperatures of -20°C and 18°C, the U-value is not impacted by the slot size.
- The U-value of energy-active window is significantly influenced by variations in supply (injected) air temperature. In order to maintain a low U-value (< 0.65 W/m^2 °C), the supply air temperature to EAW must be above the indoor temperature.
- For a window-to-floor area ratio of 10%, the EAW could potentially reduce the building heating demand by approximately 2.2 $W/m^2_{\text{floor area}}$ and 1.3 $W/m^2_{\text{floor area}}$ at outdoor temperatures of -20 °C and -5 °C, respectively. The potential increases proportionally with the window-to-floor area ratio.

Journal Pre-proof

Acknowledgement

This work is financially supported by Boverket (Swedish National Board of Housing, Building and Planning). Contributions from Uponor AB, Bravida Holding AB and KTH Live-In Lab in providing valuable information and practical support are acknowledged. The authors would also gratefully appreciate the support from Dr. Peter Platell from LOWTE AB for EAW prototyping.

References

1. Jelle BP, Arasteh D, Kohler C. State-of-the-art highly insulating window frames-research and market review project report 6-2007 SINTEF building and infrastructure. 2007.
2. Johnson T. Low-e glazing design guide, Architectural Press, ISBN-10: 0750691476, 1991.
3. Jensen KI, Schultz JM, Kristiansen FH. Development of windows based on highly insulating aerogel glazings. J. Non. Cryst. Solids 2004; 350:351–357.
4. Schultz JM, Jensen KI, Kristiansen FH. Super insulating aerogel glazing. Sol. Energy Mater. Sol. Cells 2005; 89:275–285.
5. Sun Y, Liu D, Flor JF, et al. Analysis of the daylight performance of window integrated photovoltaics systems. Renew. Energy 2020; 145:153–163.
6. Chow T tai, Li C, Lin Z. Innovative solar windows for cooling-demand climate. Sol. Energy Mater. Sol. Cells 2010; 94:212–220.
7. Han K, Kim JH. Reflectance modulation of transparent multilayer thin films for energy efficient window applications. Mater. Lett. 2011; 65:2466–2469.
8. Fang Y, Memon S, Peng J, et al. Solar thermal performance of two innovative configurations of air-vacuum layered triple glazed windows. Renew. Energy 2020; 150:167–175.
9. Manz H, Brunner S, Wullschleger L. Triple vacuum glazing: Heat transfer and basic mechanical design constraints. Sol. Energy 2006; 80:1632–1642.
10. Fang Y, Hyde TJ, Hewitt N. Predicted thermal performance of triple vacuum glazing. Sol. Energy 2010; 84:2132–2139.
11. Fang Y, Eames PC, Norton B, et al. Low emittance coatings and the thermal performance of vacuum glazing. Sol. Energy 2007; 81:8–12.
12. Jelle BP, Hynd A, Gustavsen A, et al. Fenestration of today and tomorrow: A state-of-the-art review and future research opportunities. Sol. Energy Mater. Sol. Cells 2012; 96:1–28.
13. Li D, Wu Y, Liu C, et al. Numerical investigation of thermal and optical performance of window units filled with nanoparticle enhanced PCM. Int. J. Heat Mass Transf. 2018; 125:1321–1332.

Journal Pre-proof

14. Hu Y, Guo R, Heiselberg PK. Performance and control strategy development of a PCM enhanced ventilated window system by a combined experimental and numerical study. Renew. Energy 2020; 155:134–152.

15. Hu Y, Heiselberg PK, Guo R. Ventilation cooling/heating performance of a PCM enhanced ventilated window - an experimental study. Energy Build. 2020; 214:109903.

16. Lago TGS, Ismail KAR, Lino FAM. Ventilated double glass window with reflective film: Modeling and assessment of performance. Sol. Energy 2019; 185:72–88.

17. Zeyninejad Movassag S, Zamzamian K. Numerical investigation on the thermal performance of double glazing air flow window with integrated blinds. Renew. Energy 2020; 148:852–863.

18. Zhang C, Gang W, Wang J, et al. Numerical and experimental study on the thermal performance improvement of a triple glazed window by utilizing low-grade exhaust air. Energy 2019; 167:1132–1143.

19. Michaux G, Greffet R, Salagnac P, et al. Modelling of an airflow window and numerical investigation of its thermal performances by comparison to conventional double and triple-glazed windows. Appl. Energy 2019; 242:27–45.

20. Liu M, Heiselberg PK, Larsen OK, et al. Investigation of Different Configurations of a Ventilated Window to Optimize Both Energy Efficiency and Thermal Comfort. Energy Procedia 2017; 132:478–483.

21. Lollini R, Danza L, Meroni I. Energy efficiency of a dynamic glazing system. Sol. Energy 2010; 84:526–537.

22. Casini M. Active dynamic windows for buildings: A review. Renew. Energy 2018; 119:923–934.

23. Buitrago Villaplana E. LCC and LCA for Low Temperature Heating Integrated with Energy Active Envelope Systems. 2020.

24. Schmidt D, Jóhannesson G. Model for the thermal performance of a double air gap wall construction. Nord. J. Build. Phys. 1999; 2.

25. Zhao Y, Curcija D, Power JP, et al. Improved Heat Transfer Correlations for Quantifying Laminar Natural Convection Across Fenestration Glazing Cavities. ASHRAE, Therm. Perform. Exter. Envel. Build. VII 1998; 397–403.

26. Churchill SW, Chu HHS. Correlating equations for laminar and turbulent free convection from a vertical plate. Int. J. Heat Mass Transf. 1975; 18:1323–1329.

27. Bar-Cohen A, Rohsenow WW. Thermally optimum spacing of vertical, natural convection cooled, parallel plates. J. Heat Transfer 1984; 106:116–123.

28. Bergman TL, Lavine AS. Incropera's principles of heat and mass transfer. , John Wiley &

Journal Pre-proof

Sons, ISBN: ES8-1-119-32042-5, 2017.

29. Stephan K. Heat transfer and pressure drop in undeveloped laminar flow in pipes and parallel plates (in German). Chemie Ing. Tech. 1959; 31:773–778.

30. Granryd E. Heat transfer and pressure drop in forced convection through fin arrays (in Swedish). Institutionen för Mek. Värmeteori och Kylteknink, K. Tek. Högskolan 1964.

31. Cengel YA, Ghajar AJ. Heat and Mass Trasnfer: Fundametals and Applications, McGraw-Hill, ISBN10: 0073398187, 2015.

32. Bejan A. Convection heat transfer, John Wiley & Sons, ISBN: 9781118671627, 2013.

33. Jeffreys H. The stability of a layer of fluid heated below. London, Edinburgh, Dublin Philos. Mag. J. Sci. 1926; 2:833–844.

34. Pellow A, Southwell RV. On maintained convective motion in a fluid heated from below. R. Soc. London. Ser. A, Math. Phys. Sci. 1940; 176:312–343.

35. Papanicolaou E, Jaluria Y. Mixed convection from an isolated heat source in a rectangular enclosure. Numer. Heat Transf. Part A Appl. 1991; 18:427–461.

36. Raji A, Hasnaoui M. Mixed convection heat transfer in a rectangular cavity ventilated and heated from the side. Numer. Heat Transf. Part A Appl. 1998; 33:533–548.

37. Singh S, Sharif MAR. Mixed convective cooling of a rectangular cavity with inlet and exit openings on differentially heated side walls. Numer. Heat Transf. Part A Appl. 2003; 44:233–253.

38. Rolle KC. Heat and mass transfer, Cengage Learning, Inc. ISBN10 1285178807, 2015.

39. Shah RK, London AL. Laminar flow forced convection in ducts: a source book for compact heat exchanger analytical data, ISBN-13: 978-0120200511, 1978.

40. Versteeg HK, Malalasekera W. An Introduction to Computational Fluid Dynamics. Introd. to Comput. Fluid Dyn. ISBN-10: 0470235152, 2016.

41. Larsson U, Moshfegh B, Sandberg M. Thermal analysis of super insulated windows (numerical and experimental investigations). Energy Build. 1999; 29:121–128.

42. ElSherbiny SM, Raithby GD, Hollands KGT. Heat transfer by natural convection across vertical and inclined air layers. J. Heat Transfer 1982; 104:96–102.

43. Bergman T. Double column windows, Test of function and performance (Dubbelspaltfönster Test av funktion och prestanda). 2009.

44. Boverket´s mandatory provisions and general recommendations, BBR. BFS 2011:6 with amendments up to BFS 2018:4. 2018.

Journal Pre-proof

Journal Pre-proof

Highlights:

- Thermal performance of a novel window type is investigated
- A detailed heat transfer model is developed and validated
- Waste heat is efficiently used to decrease building peak heat demands
- Suggested window type has lower transmittance than conventional equivalent

Journal Pre-proof

Journal Pre-proof

Response to Reviewers

Comments received on 2020-10-06 - Ms. Ref. No. RENE-D-20-03385

Title: Heat transfer model for energy-active windows – An evaluation of efficient reuse of waste heat in buildings

The authors are again grateful for the reviewers' comments. The minor changes requested by the first reviewer are applied in the new version.

Reviewer #1:

The authors respond to the reviewers' comments.

I have yet one recommendation: when you compare temperature profile, for example in figure 7a, please do not use percentage but difference in degrees because it is very unusual to use percentage to describe temperature changes.

- Response:
    - This is addressed in the new version.

Reviewer #2:

No further recommendations are needed.

The authors want once again to thank the reviewers for their time spent on reviewing our manuscript and for their valuable comments.

Journal Pre-proof

Declaration of interests

☒ The authors declare that they have no known competing financial interests or personal relationships that could have appeared to influence the work reported in this paper.

☐The authors declare the following financial interests/personal relationships which may be considered as potential competing interests:

Journal Pre-proof